ELSEVIER

Journal of Nuclear Materials 290–293 (2001) 362–366

journal of nuclear materials

www.elsevier.nl/locate/jnucmat

Investigation of carbon transport in the scrape-off layer of TEXTOR-94

P. Wienhold [a,*], H.G. Esser [a], D. Hildebrandt [b], A. Kirschner [a], M. Mayer [a], V. Philipps [a], M. Rubel [c]

[a] *Association EURATOM-KFA, Institut für Plasmaphysik, Forschungszentrum Jülich GmbH, P.O. Box 1913, Trilateral Euregio Cluster (TEC), D-52425 Jülich, Germany*

[b] *EURATOM Association, Max-Planck-Institut für Plasmaphysik, D-10117 Berlin, Germany*

[c] *Association EURATOM-NFR, Alfvén Laboratory, Royal Institute of Technology, S-10044 Stockholm, Sweden*

Abstract

$^{13}CH_4$ was injected into 18 consecutive ohmic discharges (108 s) through a hole in a graphite block equipped with an aluminium plate. CH and CII radical emission adjacent the hole was observed by spectroscopy, while the incremental grow of the deposit was measured in situ by colorimetry. SIMS depth profiling yielded the fractions of ^{13}C and of the ^{12}C out of the background. Ratios up to $^{13}C/C \approx 0.42$ were found although the deposition efficiency for ^{13}C was only about 0.2%. H and D were co-deposited up to ratios of 0.4 and 0.2, respectively, as measured by NRA and ERDA. The results can be simulated quantitatively by means of the ERO-TEXTOR code if high re-erosion is assumed for the hydrogen rich radicals CH_x^+. Within the interaction depth the $^{13}C/C$ ratio seems to become quasi-stationary. ^{13}C transported to obstacles creates a ratio of $^{13}C/C \approx 0.27$ after 108 s. © 2001 Elsevier Science B.V. All rights reserved.

Keywords: Carbon; Transport; Deposition; Simulation; TEXTOR-94

1. Introduction

Steady-state operation of nuclear fusion devices is one of the next goals, and the new machine generation like LHD, W7X or ITER are planned for long pulse operation. The continuous erosion from plasma facing wall components and the transport of the impurities to other locations will therefore remain a serious problem. Not only the lifetime of the components is affected, but also the tritium inventory due to co-deposition in the accumulated material. This is mainly carbon, but also boron, tungsten, beryllium, steel components and oxygen. The deposits can form flakes and dust and are usually difficult to access [1,2] as has been shown in several machines (TEXTOR-94 [3], ASDEX-U [4]), JET [5]). Flakes with thicknesses in the range 10–100 μm are observed in the divertor region, especially in shadowed areas, but also in the main chamber near the LCFS on plasma facing surfaces, and on areas deep in the shadow [6]. Because carbon-based components are still used the investigation of the transport of carbon as the major impurity remains an important issue. In particular, the application of ^{13}C as a 'tracer' impurity allows to investigate carbon transport in a ^{12}C surrounding and may become beneficial also for other machines. Of special interest were simulation calculations with the ERO-TEXTOR code [7] which lead to a better understanding of the deposition and re-erosion process. The emphasis of the paper is therefore put on the discussion of the processes. Part of the observations have already been published [8,9].

2. Experimental

For the experiment, a graphite block (dimensions: $115 \times 75 \times 70$ mm^3) was positioned in the scrape-off

* Corresponding author. Tel.: +49-2461 61 3203; fax: +49-2461 61 2660.

E-mail address: p.wienhold@fz-juelich.de (P. Wienhold).

0022-3115/01/$ - see front matter © 2001 Elsevier Science B.V. All rights reserved.
PII: S0022-3115(00)00573-0

layer (SOL) with its outer end at the last closed flux surface (LCFS, $r = 46$ cm). The surface of the block was covered with an aluminium target plate ($108 \times 70 \times 3$ mm^3). This plate was inclined by 20° in toroidal direction such that the end reached the distance $r = 50$ cm (Fig. 1). It was kept there for 20 discharges ($n_e = 2.5 \times 10^{13}$ cm^{-3}, $I_p = 350$ kA, $B_T = 2.25$ T, total exposure time 107.7 s) in deuterium without auxiliary heating. No gas was injected during the first two discharges, while in the following 18 discharges injection of $^{13}CH_4$ through a hole (∅1.7 mm) began at 1 s with the calibrated amount of 3.8 mbarℓ (9.2×10^{19} molecules). The CH and CII light emitted between surface and plasma edge was observed in poloidal direction. Both reached maximum at 1.26 s after discharge began and levelled off after 2 s. Fig. 1 shows that the CH light emission was brightest at the LCFS ($r \approx 46$ cm) and near the location of the blowing hole (white spot). CII radiated brightest at $r \approx 45$ cm.

The ^{13}C penetrated partly into the plasma and increased the CV signal by ≈33%. The rest became redeposited on the target plate together with ^{12}C carried by the SOL plasma. Because hydrogen was co-deposited, a transparent film was formed the thickness of which was measured by colorimetry [10]. Fig. 2 shows the interference fringes on the target plate after dismounting. The orders can be counted up to the 3rd (≈300 nm) from left to right. Note, that each toroidal location corresponds to another radial distance from the plasma centre. At the left side ('plasma far') the deposition is mainly due to the ^{12}C in the SOL. The colour contours show little variation in poloidal direction. The thickness increases at the plasma near the side (right) because the background flux increases. Beyond the blowing hole the contours are bent back due to the additional ^{13}C deposition, resulting into a 'butterfly' like pattern. This area of additional ^{13}C deposition is shifted poloidally by about 6 mm (circle) due to the ExB forces. Other areas are almost unaffected by ^{13}C, and the deposition is mainly due to ^{12}C. This was found by secondary ion mass spectroscopy (SIMS) along the dotted line. Nuclear reaction analysis (NRA) and elastic recoil detection analysis (ERDA) were applied in order to determine the co-deposited deuterium and hydrogen (white line). Additionally, an aluminium sample was mounted perpendicular to the toroidal direction well in the shadow of the puffed molecular $^{13}CH_4$ cloud (see Fig. 1). The deposits found here were formed mainly by the impurities travelling in the SOL.

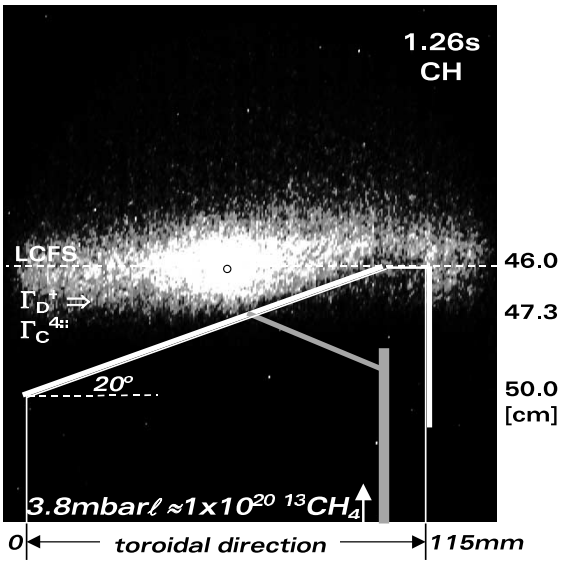

Fig. 1. CH light during $^{13}CH_4$ puffing in poloidal view in the moment of maximum brightness (1.26 s). The spot indicates the location of highest intensity. The inclined graphite block, the blowing hole, and the Al targets are shown in schematically.

3. Results

3.1. Deposition efficiency

The fringe shifts which were observed by a camera after each of the puffs yield the incremental growth of the thickness and, hence, the deposition rates at the different locations. But, mainly a bean-like region of about 8.7 cm^2 was affected by the additional deposition of the ^{13}C. This became pronouncedly visible in the false colour representations of the images (see Fig. 1 in [11]). Those images were also used in order to estimate the thickness profiles along two lines which intersected the areas where mainly ^{12}C or ^{13}C+^{12}C were deposited, respectively. The differences yield the ^{13}C contribution alone [8,9]. The average deposition efficiency yielded from the 18 single measurements is only $0.2\% \pm 0.1\%$.

3.2. Isotopic ratios of carbon and hydrogen

Depth profiling combined with SIMS analysis applied at 13 equidistant locations yields not only the total thickness of the deposit, but also the ratio $^{13}C/^{12}C$ within the layer and, hence, the contributions of the two isotopes separately. The results are given in Fig. 3. For example, ^{13}C contributes with a thickness of ≈100 nm at distances 2–4 cm from the blowing hole (black columns), while ^{12}C (white columns) delivers ≈200 nm. The sum fully agrees with the total thickness determined by colorimetry (not shown). Obviously, ^{13}C has been transported several cm across the declined surface in toroidal direction towards the plasma near end of the target. The concentration $^{13}C/C = {}^{13}C/({}^{13}C+{}^{12}C)$ is not constant, however, and reaches 0.42 near the blowing hole. The decrease to ≈0.25 with increasing distance might

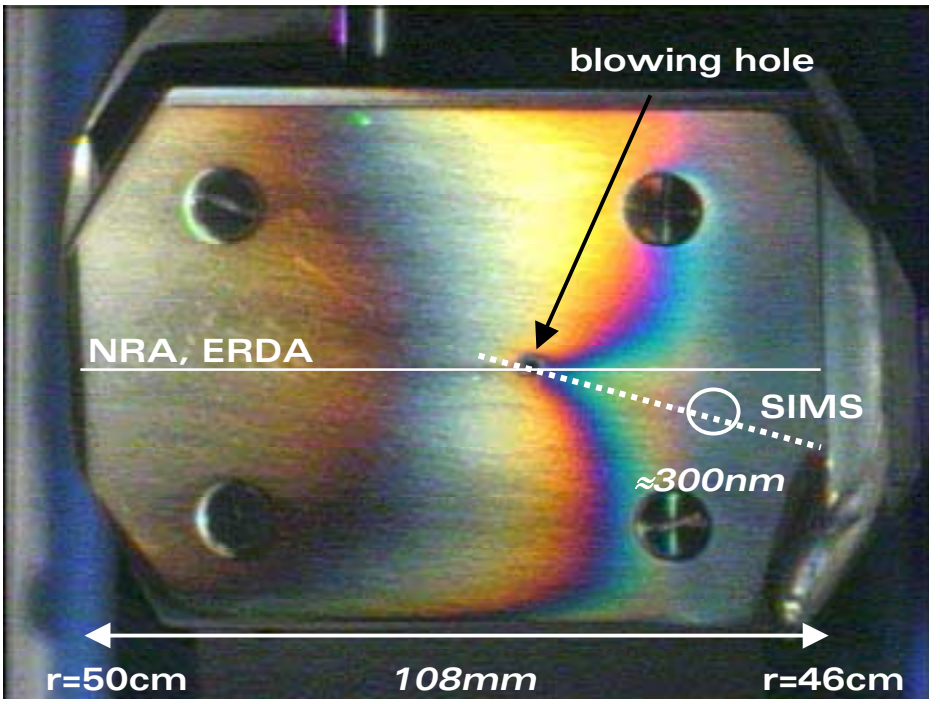

Fig. 2. Top view on the inclined aluminium target plate after dismounting. The interference colours indicate increasing thickness from left to right (toroidal direction). The lines of ion beam analyses are indicated.

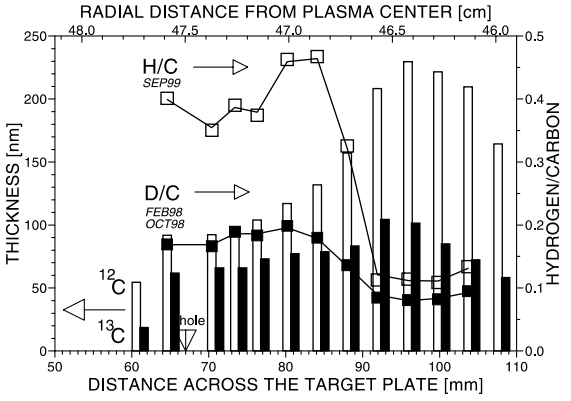

Fig. 3. Contribution of ^{13}C (black columns) and ^{12}C (white columns) to the thickness as determined from SIMS depth profiling at 13 different locations. ERDA in combination with NRA yielded in the ratios H/C (open squares) and D/C (full squares).

indicate the limited local transport. The slight decrease in thickness beyond the maximum at $r = 46.5$ cm is likely due to the increasing erosion by D^+ ions.

Deuterium is co-deposited with ratios D/C ≈0.2 rather independent on distance as found by NRA (full squares). Hydrogen from the injected molecules is co-deposited up to ratios H/C ≈0.45 revealed by ERDA (open squares). Both values drop to ≈0.1 adjacent to the end of the target plate (r ≈46 cm) due to the temperature excursions.

4. Discussion

4.1. Simulation calculations

The very low deposition efficiency of less than 1% highly disagrees with the expectations from the spectroscopic observations. As Fig. 1 shows the maximum of the CH light emission occurs at the LCFS just above the target. Since most of the $^{13}CH_4$ molecules have to break up and become ionised within that small gap in order to reach the CH stage, a high fraction of them must travel along the magnetic field lines towards the declined target plate. They should become deposited and cause a high deposition efficiency. This is obviously not the case and points to the direction that the re-erosion probability of the CH_x radicals is very high.

To prove this idea simulations with the ERO-TEXTOR Monte-Carlo code were performed. This code models the local transport and re-deposition of eroded impurities. The ion flux ($\Gamma_D^+ = 1.33 \times 10^{19}$ cm^{-2} s^{-1}, $\Gamma_C^{4+} = 0.036\Gamma_D^+$, $\lambda_D = 17$ mm) hitting the declined surface is assumed to liberate CD_4 or C by chemical and

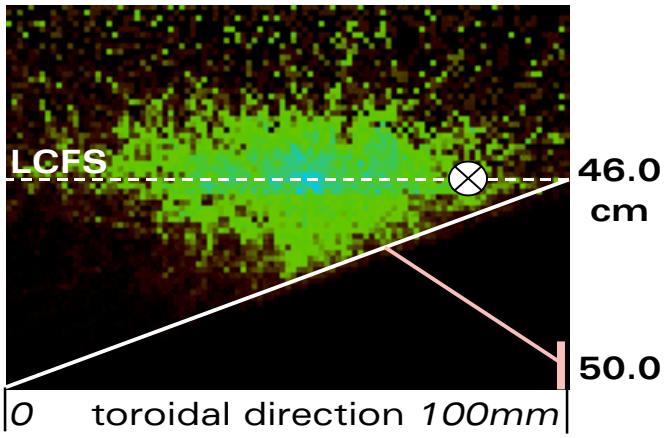

Fig. 4. Two-dimensional pattern of the CH emission light as simulated by means of the ERO-TEXTOR code for 'high' re-erosion probability of the ionic fractions. Maximum emission (blue zone) is shifted to a location not observed (white cross) if thermal energy is assumed for the re-eroded species.

physical erosion. The intermittent injection was replaced by a constant inlet rate of 1.5×10^{19} s^{-1} of thermal $^{13}CH_4$ molecules. After ionisation they travel either back to the declined surface or leave the simulation volume. It is assumed that only ions stick and change the ratio $^{13}C/^{12}C$ within an interaction depth of $\Delta = 40$ nm. Neutral hydrocarbons do not contribute. Outputs as the ^{13}C pattern or the DH light emission can directly be compared with experimental observations. Usually, 50% of the ionised radicals hitting the surface are assumed to stick, the rest leaves it in the form of $^{13}CH_4$. This is described by a 'reflection coefficient' $R_{ion} = 0.5$. This assumption leads, however, to insuperable disagreements with the experimental results: The efficiency for ^{13}C deposition reaches 40% and causes thicknesses of 80–160 μm adjacent the hole while in the experiment a maximum of 0.3 μm was found several cm away. The concentration $^{13}C/C$ approaches unity in contrary to the experiment (0.42).

Obviously, the high sticking probability assumed for the $^{13}CH_x^+$ radicals is responsible for the huge ^{13}C deposition. Varying other input parameters, such as density, puffing rate, sputter yields, ionisation probabilities, did not lower the value sufficiently. But, if a direct re-erosion was assumed optimum agreement was found with all experimental findings. This case was simulated by setting $R_{ion} = 1$. It reduced the efficiency to 2.5%, lowered $^{13}C/C$ to 0.5, shifted the maximum to the right location, and calculated correctly the ^{13}C pattern. The maximum thickness of 1.6 μm is still ≈5 times too high. Possibly, erosion by oxygen impurity ions or by hydrogen released from the hydrocarbons, which were not taken into account, decreased the thickness in the experiment. In addition, the calculated toroidal and radial distributions for the CH and CII light agree well with the measured ones. As illustration the calculated CH emission is given in Fig. 4 and shows the agreement with the experimentally observed (see Fig. 1).

The process of 'high re-erosion' is, however, not fully understood. It can mean, that the initial radicals (CH_4^+ and CH_3^+) which return to the surface after travelling a short radial distance carry too little energy to form a stable deposit. Increased erosion by hydrogen is e.g. observed when a-C:H films are formed in glow discharges with self-bias voltages below 200 eV [12]. Probably the surplus of hydrogen carried by the radicals causes the high re-erosion. It seems that the re-eroded hydrocarbon leaves the surface with more than thermal energy. For thermal energy the maximum emission would have been shifted toroidally by 30 mm (cross).

4.2. Carbon transport in TEXTOR-94

More than 99% (1.66×10^{21} molecules) of the introduced ^{13}C are deposited at other locations inside the machine, most likely on the graphite tiles of the toroidal belt limiter ALTII (3.4 m^2). This amount would correspond to a thickness of 7.5 nm and should create a ratio $^{13}C/C \approx 0.2$ provided $\Delta = 40$ nm. Because of the co-deposition of ^{12}C a mixed layer will be formed. This shows schematically Fig. 5. Since these are net erosion zones the mixture is re-eroded, however, and feeds the carbon flux in the SOL with the according isotopic ratio. The re-deposition will eventually end on obstacles.

If such a perception is true, these deposits should show an carbon isotopic ratio independent of the radial distance from the plasma centre. This was indeed discovered on the target mounted perpendicular to the toroidal direction (Fig. 1). Fig. 6 summarises the results found by SIMS depth profiling. Despite the increase of the thickness (crosses) of the deposit up to 1 μm, the ratio $^{13}C/C \approx 0.27$ remains constant (boxes). In contrast,

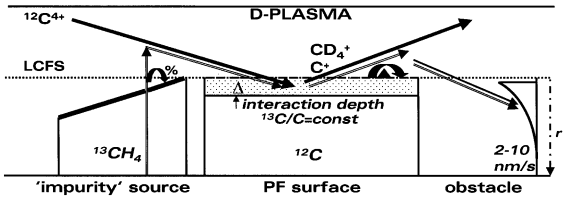

Fig. 5. Schematic of the carbon transport in TEXTOR. Erosion and deposition affect the 'interaction depth' Δ of the plasma facing surfaces. Net transport ends on obstacles in the SOL or on self-shadowed areas of PFC's.

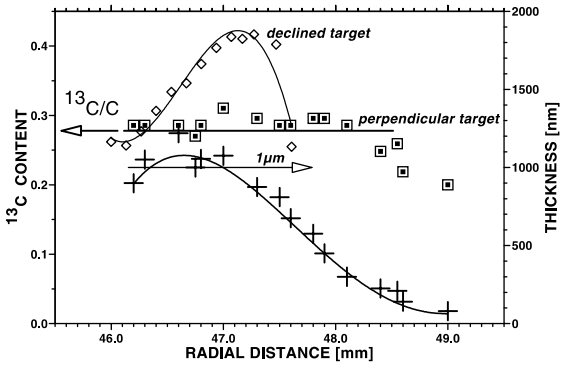

Fig. 6. ^{13}C concentration (boxes) and thickness of the deposit (crosses) as found by SIMS depth profiling and colorimetry on the target mounted perpendicular to the toroidal direction. For comparison $^{13}C/C$ on the declined target is also given (diamonds).

the ratio increases up to 0.42 on the declined target (diamonds) where the molecules were injected. The constant ratio $^{13}C/C \approx 0.27$ suggests that quasi-stationarity is achieved and corresponds to an interaction depth $\Delta \approx 27$ nm if the limiter area is taken into account. This is likely a lower limit, because the limiter exhibits a complicated pattern of erosion and deposition regions, which is caused by the magnetic field ripple and the complex shape. Only roughly one half of the area shows net erosion, the other half net deposition. The thickness of 1 μm achieved after 107.7 s ($\approx$10 nm s^{-1} at $r \approx 46$ cm) indicates an average carbon flux of 1.5×10^{19}/s which is permanently transported from the limiters via the SOL to the sinks. This drives the formation of flakes of thicknesses in the 100 μm range in areas not further affected by erosion [13].

5. Conclusions

Since the local carbon transport and re-deposition not only depend on plasma parameters, but also sensitively on other circumstances like magnetic field ripple and shape or orientation of the wall components, predictions are difficult to make. Investigations have to be done individually in the different machines. The use of $^{13}CH_4$ can be beneficial because ^{13}C behaves like a 'tracer' impurity in a surrounding of mainly ^{12}C. But it seems that for long pulse operation erosion and deposition in the steady state are characterised by constant rates unequal to zero. The process of enhanced re-erosion suggested is not fully understood yet and needs further investigation. The ERO-TEXTOR code which has been shown to simulate correctly the local transport phenomena will therefore be a helpful tool.

Acknowledgements

The authors had great scientific support from M. Lehnen and F. Weschenfelder. They are very thankful for technical assistance by M. Freisinger, W. Müller and H. Reimer.

References

[1] M. Mayer, R. Behrisch, K. Plamann et al., J. Nucl. Mater. 266–269 (1999) 604.
[2] M. Mayer, R. Behrisch, P. Andrew et al., Physica Scripta T 81 (1999) 13.
[3] P. Wienhold, H.G. Esser, D. Hildebrandt et al., Physica Scripta T 81 (1999) 19.
[4] H. Maier et al., in: Proceedings of the 26th EPS Conference on Controlled Fusion in Plasma Physics, 14–18 June 1999, Maastricht, The Netherlands.
[5] P. Andrew, D. Brennan, J.P. Coad et al., J. Nucl. Mater. 266–269 (1999) 153.
[6] J. Von Seggern, M. Rubel, P. Karduck et al., Physica Scripta T 81 (1999) 31.
[7] A. Kirschner, V. Philipps, A. Pospieszczik et al., in: Proceedings of the 26th EPS Conference on Controlled Fusion in Plasma Physics, 14–18 June 1999, Maastricht, The Netherlands.
[8] P. Wienhold, H.G. Esser, D. Hildebrandt et al., in: Proceedings of the 26th EPS Conference on Controlled Fusion in Plasma Physics, 14–18 June 1999, Maastricht, The Netherlands.
[9] P. Wienhold, D. Hildebrandt, A. Kirschner et al., in: Proceedings of the 10th International Toki Conference on Plasma Physics and Controlled Fusion, 18–21 January 2000, Toki City, Japan.
[10] P. Wienhold, F. Weschenfelder, J. Winter, NIMB in Phys. Res. B 94 (1994) 503.
[11] A. Kirschner, V. Philipps, P. Wienhold, J. Winter, these Proceedings.
[12] E. Vietzke et al., in: E-MRS Meeting, vol. 17, June 1987, p. 351.
[13] M. Rubel, P. Wienhold, D. Hildebrandt, these Proceedings.